Journal of Statistical Physics, Vol. 46, Nos. 3/4, 1987

On the Critical Behavior of the Ising Model with Mixed Two- and Three-Spin Interactions

Francisco C. Alcaraz[1,2] **and Michael N. Barber**[1,3]

Received July 31, 1986

A study is made of a two-dimensional Ising model with staggered three-spin interactions in one direction and two-spin interactions in the other. The phase diagram of the model and its critical behavior are explored by conventional finite-size scaling and by exploiting relations between mass gap amplitudes and critical exponents predicted by conformal invariance. The model is found to exhibit a line of continuously varying critical exponents, which bifurcates into two Ising critical lines. This similarity of the model with the Ashkin–Teller model leads to a conjecture for the exact critical indices along the nonuniversal critical curve. Earlier contradictions about the universality class of the uniform (isotropic) case of the model are clarified.

KEY WORDS: Ising models; finite-size scaling; critical phenomena; multispin interactions; conformal invariance; Ashkin–Teller model; Potts models.

1. INTRODUCTION

Ising models with multispin interactions are known to exhibit a rich variety of critical behavior. The classical examples in two dimensions are the eight-vertex model[1] and the Ashkin–Teller model,[2] both of which may be formulated as Ising models with two- and four-spin interactions,[3] and the Baxter–Wu model,[4] which is an Ising model with three-spin interactions around each elementary face of a triangular lattice. Although these models are formulated in terms of Ising $[Z(2)]$ variables, their multispin interac-

[1] Department of Mathematics, Faculty of Science, Australian National University, Canberra, A.C.T. 2601, Australia.

[2] Permanent address: Depto de Física, Universidade Federal de São Carlos, 13560 São Carlos, SP, Brazil.

[3] Present address: Institute for Theoretical Physics, University of California, Santa Barbara, California.

0022-4715/87/0200-0435$05.00/0

tions render the relevant nonlocal symmetry $Z(2)\otimes Z(2)$. Consequently, the Baxter–Wu model is believed to belong to the same universality class as the four-state Potts model,[3,5] while the eight-vertex and Ashkin–Teller models exhibit critical lines along which the critical indices vary continuously with the multispin coupling.[3] In the Ashkin–Teller model, but not in the eight-vertex model, this line ultimately bifurcates into two Ising critical lines; the bifurcation point corresponding to the four-state Potts model.[3,6]

In this paper we introduce and study an Ising model that shows the same richness as the Ashkin–Teller model but has only two- and three-spin couplings. The model is an extension of the three-spin Ising model proposed by Debierre and Turban[7] (see also Penson *et al.*[8]). Various investigations of the critical behavior of this model have been contradictory. Our generalization was motivated by the idea that these contradictions could be resolved by viewing the behavior in a wider parameter space. As we shall see, this expectation is fruitfully borne out. The model is defined explicitly in the next section, where we also show that it is self-dual. In Sections 3 and 4 we obtain the row-to-row transfer matrix and take a "τ-continuum limit" to define a quantum Hamiltonian. Section 5 is dedicated to the study of this quantum Hamiltonian by standard finite-size scaling; we obtain the phase diagram and the critical exponent ν. In Section 6, we exploit consequences of conformal invariance of the infinite system to refine our estimates of critical exponents and to estimate the conformal anomaly number c. The paper closes with a general discussion and summary of our results in Section 7.

2. THE MODEL

Consider a two-dimensional square lattice divided into three sublattices denoted by $\bigcirc$, $\square$, and $\diamond$, as in Fig. 1. Each lattice site, labeled by an integer pair (i, j), is populated by an Ising variable $\sigma(i, j) = \pm 1$. We consider three-spin interactions in the x direction (which for future convenience we refer to as the spatial dimension) and two-spin interactions in the y direction (temporal dimension). These interactions are allowed to be "staggered" with one sublattice distinguished. The Hamiltonian of interest is then

$$-\beta H = \sum_{(i,j)} (H^x_{3i,j} + H^x_{3i,j}) \tag{2.1}$$

where

$$H^x_{ij} = K_0 \sigma(i, j)\, \sigma(i+1, j)\, \sigma(i+2, j) + K_1 \sigma(i+1, j)\, \sigma(i+2, j)\, \sigma(i+3, j) + K_1 \sigma(i+2, j)\, \sigma(i+3, j)\, \sigma(i+4, j) \tag{2.2}$$

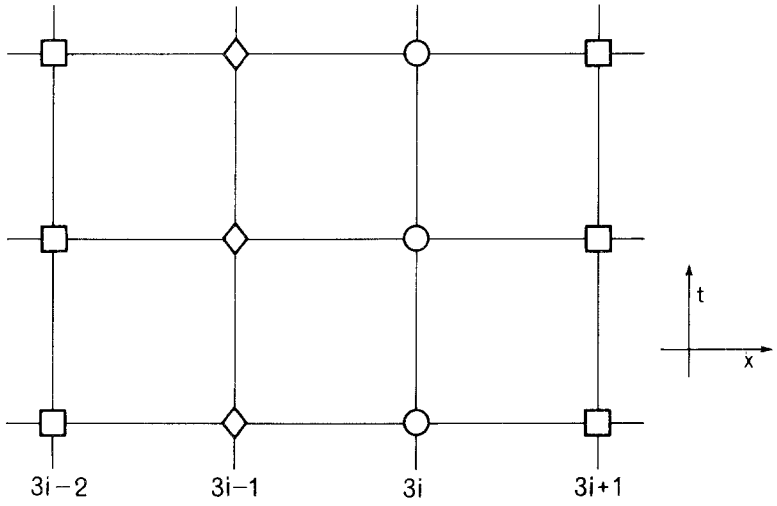

Fig. 1. Sublattices used to define model (2.1).

and

$$H'_{ij} = K'_1 \sigma(i, j)\, \sigma(i, j+1) + K'_0 \sigma(i+1, j+1)\, \sigma(i+1, j) + K'_1 \sigma(i+2, j)\, \sigma(i+2, j+1) \tag{2.3}$$

where $K_0 = \beta J_0$, $K_1 = \beta J_1$ ($K'_0 = \beta J'_0$, $K'_1 = \beta J'_1$) are the couplings in the space (time) direction, all couplings being ferromagnetic. The model is invariant under a nonlocal symmetry, which corresponds to a global $Z(2)$ transformation of any two sublattices. As a consequence of this $Z(2) \otimes Z(2)$ symmetry, the ground state is fourfold degenerate. The possible ground states are shown schematically in Fig. 2 and we shall refer to these states as (a), (b), (c), (d) as indicated in the figure.

This ground-state degeneracy is identical to that found in the Ashkin–Teller model defined by the Hamiltonian[3,6]

$$-\beta H = \sum_{\langle i, j \rangle} [K_2(\sigma_i \sigma_j + \tau_i \tau_j) + K_4 \sigma_i \sigma_j \tau_i \tau_j] \tag{2.4}$$

where $K_2 = \beta J_2$, $K_4 = \beta J_4$ are the coupling constants and the sum is over all bonds of a square lattice, the sites of which are populated by a *pair* ($\sigma = \pm 1$, $\tau = \pm 1$) of Ising spins.

A further similarity between (2.1) and the Ashkin–Teller model is revealed if we calculate the (zero-temperature) energies of possible domain walls between the different ground states. For each pair of ground states,

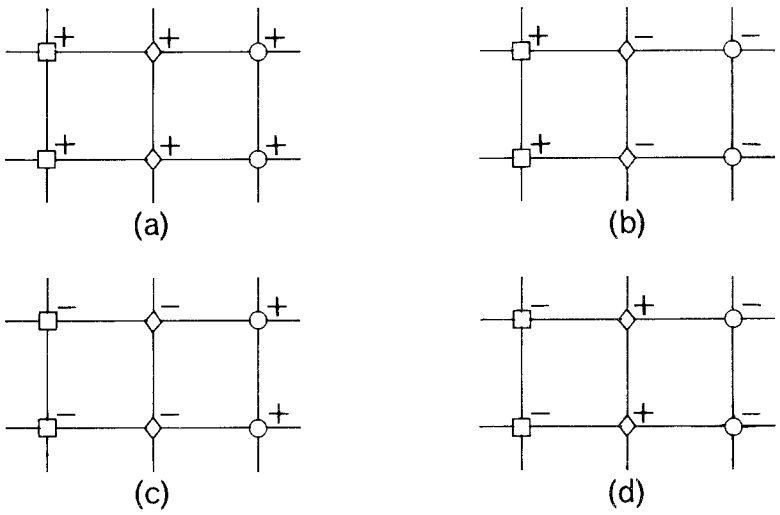

Fig. 2. Ground states of model (2.1).

three different walls can be distinguished by the location of the wall relative to the underlying sublattices (see Table I). Since two sublattices (○ and ◇) are equivalent, two of the walls have the same energy, with the third wall "heavier" or "lighter" depending on the relative values of J_0 and J_1. If we single out one of the phases, say (a), as a reference phase, then the energy of the *lowest* energy walls between the reference phase and the other phases can be summarized as in Fig. 3a. We observe that there is a quantitative change in the relative energies of the domain walls and hence presumably in low-temperature excitations of the system when $J_1 = J_0$.

The possible significance of this observation can be seen if we similarly depict (Fig. 3b) the energies of domain walls in the Ashkin–Teller model (2.4). Again we observe the quantitative change in the relative energies of domain walls that occurs when $J_2 = J_4$, a change that in this case corresponds to a radical change in the phase diagram of the model. We shall confirm in Section 5 that this similarity between the low-temperature excitations of (2.1) and those of the Ashkin–Teller model does extend to definite similarities in the phase diagrams and critical behavior of the two models.

Two particular cases of the Hamiltonian (2.1) deserve a few additional comments. The first is the case K_0, $K_0' \to \infty$, which freezes spins on sublattice □ and leads to two decoupled Ising models. This point in the phase diagram of (2.1) is consequently expected to be the analogue of the point where the four-spin coupling vanishes in the Ashkin–Teller model. The

Table I. Domain Wall Configurations of Model (2.1)

Coexisting phases (see Fig. 1)	Spin configuration[a]										Energy
	□	◇	○		□	◇		○	□	◇	○	
	+	+	+	‖	+	−		−	+	−	−	$2J_0$
a, b	+	+	+		+	−	‖	−	+	−	−	$2J_0$
	+	+	+		+	+	‖	−	+	−	−	$4J_1$
	+	+	+	‖	−	−		+	−	−	+	$2J_1$
a, c	+	+	+		+	−	‖	+	−	−	+	$2J_0 + 2J_1$
	+	+	+		+	+	‖	+	−	−	+	$2J_1$
	+	+	+	‖	−	+		−	−	+	−	$2J_0 + 2J_1$
a, d	+	+	+		+	+	‖	−	−	+	−	$2J_1$
	+	+	+		+	+	‖	−	−	+	−	$2J_1$
	+	−	−	‖	−	−		+	−	−	+	$2J_0 + 2J_1$
b, c	+	−	−		+	−	‖	+	−	−	+	$2J_1$
	+	−	−		+	−	‖	+	−	−	+	$2J_1$
	+	−	−	‖	−	+		−	−	+	−	$2J_1$
b, d	+	−	−		+	+	‖	−	−	+	−	$2J_0 + 2J_1$
	+	−	−		+	−	‖	−	−	+	−	$2J_1$
	−	−	+	‖	−	+		−	−	+	−	$2J_0$
c, d	−	−	+		−	+	‖	−	−	+	−	$2J_0$
	−	−	+		−	−	‖	−	−	+	−	$4J_1$

[a] ‖ marks the location of the wall.

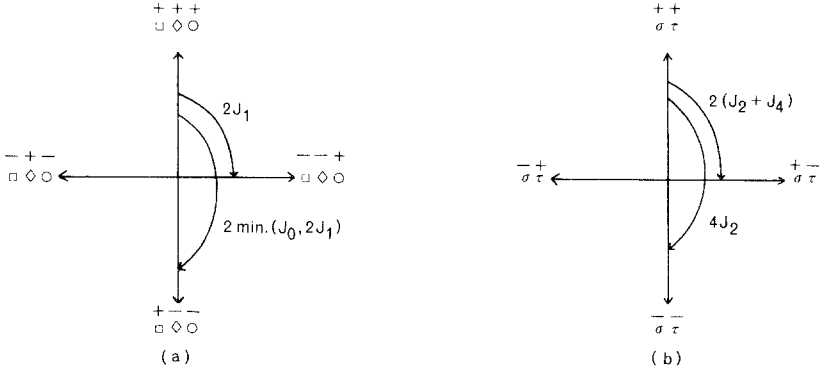

Fig. 3. Relative domain wall energies for (a) model (2.1), (b) Ashkin–Teller model.

second special case is obtained by setting $K_0 = K_1$, $K_0' = K_1'$, which reduces (2.1) to the three-spin Ising model introduced by Debierre and Turban[7] (see also Penson *et al.*[8] and Turban[9]). Figure 3 suggests that this limit corresponds to the point at which the Ashkin–Teller model reduces to the four-state Potts model. This correspondence supports the conjecture[8,9] that the spatially uniform model belongs to the same universality class as the four-state Potts model. Direct finite-lattice calculations[7,8,10] on this uniform model have been contradictory, although a recent, more detailed analysis[11] did add support to the conjecture. Nevertheless, a study of the extended model (2.1), particularly in comparison with the Ashkin–Teller model, should shed additional light on the nature of criticality in the uniform model.

3. TRANSFER MATRIX AND DUALITY TRANSFORMATION

The row-to-row transfer matrix T for the model (2.1) is easily derived by standard methods (see, e.g., Ref. 12). We write

$$T(K_0, K_1, K_0', K_1') = T_1 \cdot T_2 \tag{3.1}$$

with

$$T_1 = \prod_{i=-\infty}^{\infty} \exp(K_0 \sigma_{3i}^z \sigma_{3i+1}^z \sigma_{3i+2}^z + K_1 \sigma_{3i+1}^z \sigma_{3i+2}^z \sigma_{3i+3}^z + K_1 \sigma_{3i+2}^z \sigma_{3i+3}^z \sigma_{3i+4}^z) \tag{3.2}$$

and

$$T_2 = \prod_{i=-\infty}^{\infty} c_0 c_1^2 \exp(V_1' \sigma_{3i}^x + V_0' \sigma_{3i+1}^x + V_1' \sigma_{3i+2}^x) \tag{3.3}$$

where σ_i^x and σ_i^z are Pauli spin matrices. The new constants are related to the old coupling constants through

$$V_0' = -\frac{1}{2} \ln \tanh K_0', \qquad V_1' = -\frac{1}{2} \ln \tanh K_1'$$
$$c_0 = (2 \sinh 2K_0')^{1/2}, \qquad c_1 = (2 \sinh 2K_1')^{1/2} \tag{3.4}$$

To perform a dual transformation on (2.1), we define dual variables[7,9]

$$\tilde{\sigma}_i^x = \sigma_i^z \sigma_{i+1}^z \sigma_{i+2}^z, \qquad \tilde{\sigma}_i^z = \prod_{k \geqslant 0} \sigma_{i-3k}^x \sigma_{i-3k-1}^x \tag{3.5}$$

which obey the same algebra as the original Pauli matrices. Inverting, we can write

$$\sigma_i^x = \tilde{\sigma}_{i-2}^z \tilde{\sigma}_{i-1}^z \tilde{\sigma}_i^z \tag{3.6}$$

In terms of these new dual variables, the transfer matrix is still given by (3.1), but with

$$T_2 = \prod_{i=-\infty}^{\infty} c_0 c_1^2 \exp(V_0' \tilde{\sigma}_{3i}^z \tilde{\sigma}_{3i+1}^z \tilde{\sigma}_{3i+2}^z + V_1' \tilde{\sigma}_{3i+1}^z \tilde{\sigma}_{3i+2}^z \tilde{\sigma}_{3i+3}^z + V_1' \tilde{\sigma}_{3i+2}^z \tilde{\sigma}_{3i+3}^z \tilde{\sigma}_{3i+4}^z) \tag{3.7}$$

$$T_1 = \prod_{i=-\infty}^{\infty} \exp(K_1 \tilde{\sigma}_{3i}^x + K_0 \tilde{\sigma}_{3i+1}^x + K_1 \tilde{\sigma}_{3i+2}^x) \tag{3.8}$$

Comparison of (3.2), (3.3) and (3.7), (3.8) shows that (2.1) is self-dual,[7,13,14] the dual transformation simply relating two different points in the parameter space:

$$T(K_0, K_1, V_0', V_1') = T(V_0', V_1', K_0, K_1) \tag{3.9}$$

The self-dual surface (fixed under the duality transformation) follows by equating $K_0 = V_0'$; $K_1 = V_1'$. Hence, from (3.4) the self-dual surface is given by

$$e^{-2K_0} = \tanh K_0', \qquad e^{-2K_1} = \tanh K_1' \tag{3.10}$$

4. QUANTUM HAMILTONIAN LIMIT

Instead of working directly with model (2.1), we will base our analysis on a "τ-continuum" limit[12,15] of the transfer matrix, which corresponds to a quantum Hamiltonian in $(1+1)$ dimensions with "time" continuous. The well-known advantages of this formalism are the resulting one-dimensional geometry of the problem and, particularly from a numerical point of view, the fact that the Hamiltonian is a sparse matrix compared to the transfer matrix, which is dense.

The two-dimensional classical model (2.1) is reduced to a $(1+1)$-dimensional quantum model by taking the extreme anisotropic limit $(K_0, K_1) \to 0$, $(K_0', K_1') \to \infty$. This limit can be performed in several ways. Following the analogous treatment[16] of the Ashkin–Teller model, we choose the particular parametrization

$$K_0 = \tau, \qquad K_1 = \alpha\tau \tag{4.1a}$$

$$\exp(-2K_0') = \lambda\tau, \qquad \exp(-2K_1') = \lambda\alpha\tau \tag{4.1b}$$

and force $\tau \to 0$ with λ and α held constant. In this limit the transfer matrix (3.1)–(3.3) can be written as

$$T = 1 - \tau H + O(\tau^2) \tag{4.2}$$

where H is the required quantum Hamiltonian given by

$$-H(\lambda, \alpha) = \sum_i [(\sigma^z_{3i}\sigma^z_{3i+1}\sigma^z_{3i+2} + \alpha\sigma^z_{3i+1}\sigma^z_{3i+2}\sigma^z_{3i+3} + \alpha\sigma^z_{3i+2}\sigma^z_{3i+3}\sigma^z_{3i+4}) + \lambda(\alpha\sigma^x_{3i} + \sigma^x_{3i+1} + \alpha\sigma^x_{3i+2})] \tag{4.3}$$

The parametrization (4.1) has the virtue of simplifying the self-dual curve, which now becomes $\lambda = 1$ with α a free parameter, exactly as occurs in the quantum Hamiltonian limit of the Ashkin–Teller model.[16] The dual transformation (3.5) can also be applied directly to the Hamiltonian (4.3), yielding

$$H(\lambda, \alpha) = \frac{1}{\lambda} H\left(\frac{1}{\lambda}, \alpha\right) \tag{4.4}$$

This implies that the critical point for all α should occur at $\lambda = 1$ provided the transition is unique.

5. FINITE-SIZE SCALING

To explore the critical behavior of (4.3), we have applied finite-size scaling techniques.[17,18] The method is by now standard. The first step is the calculation of low-lying eigenenergies of (4.3) on a finite chain of L sites with periodic boundary conditions. To preserve the symmetry of the model, we require L to be a multiple of three.

The ensuing finite-size scaling analysis is clarified if we choose as a basis for the matrix representation of H one in which all σ^x_i $(i = 1, 2, \ldots, L)$ are diagonal. In this basis, the Hilbert space associated with H separates into disjoint sectors labeled the eigenvalues of the "parity" operators

$$\mathscr{P}_1 = \prod_{i=1}^{L/3} \sigma^x_{3i}\sigma^x_{3i+1}, \qquad \mathscr{P}_2 = \prod_{i=1}^{L/3} \sigma^x_{3i}\sigma^x_{3i+2}, \qquad \mathscr{P}_3 = \mathscr{P}_1 \cdot \mathscr{P}_2 \tag{5.1}$$

which independently commute with H for all λ and α.

On a finite chain the ground-state energy $E_0(+\,+)$ of (4.3) is the energy of the lowest lying state in the sector $\mathscr{P}_1 = +$, $\mathscr{P}_2 = +$ (henceforth denoted the ground-state sector). As a consequence of the equivalence of the two sublattices $\bigcirc$ and $\diamond$, the sectors $(\mathscr{P}_1 = +, \mathscr{P}_2 = -)$ and

($\mathscr{P}_1 = -, \mathscr{P}_2 = +$) are degenerate. We may thus define two different mass gaps for the model:

$$G_L^1(\lambda, \alpha) = E_0(+-) - E_0(++), \qquad G_L^2(\lambda, \alpha) = E_0(--) - E_0(++) \tag{5.2}$$

where $E_0(+-)$ and $E_0(--)$ are the energies of the lowest lying states in the sectors ($\mathscr{P}_1 = +, \mathscr{P}_2 = -$) and ($\mathscr{P}_1 = -, \mathscr{P}_2 = -$), respectively.

The phase diagram can now be explored by applying phenomenological renormalization[17,18] to these gaps. For fixed α, we estimate the critical coupling λ_c by extrapolating the sequence of values of $\lambda_c^i(L)$ obtained by solving

$$LG_L^i(\alpha, \lambda)/(L-3)\, G_{L-3}^i(\alpha, \lambda) = 1, \qquad i = 1, 2 \tag{5.3}$$

If the infinite system has a unique phase transition, both sequences should converge to the self-dual point $\lambda_c = 1$, while if there are two phase transitions, associated with the two mass gaps G^1 and G^2 closing separately, the two sequences should converge to different points λ_c^1 and λ_c^2 such that, by duality, $\lambda_c^1 \lambda_c^2 = 1$. Estimates for the critical curve in the α–λ parameter space obtained by using lattices of size $L = 6, 9, 12$ in (5.3) are shown in Fig. 4,

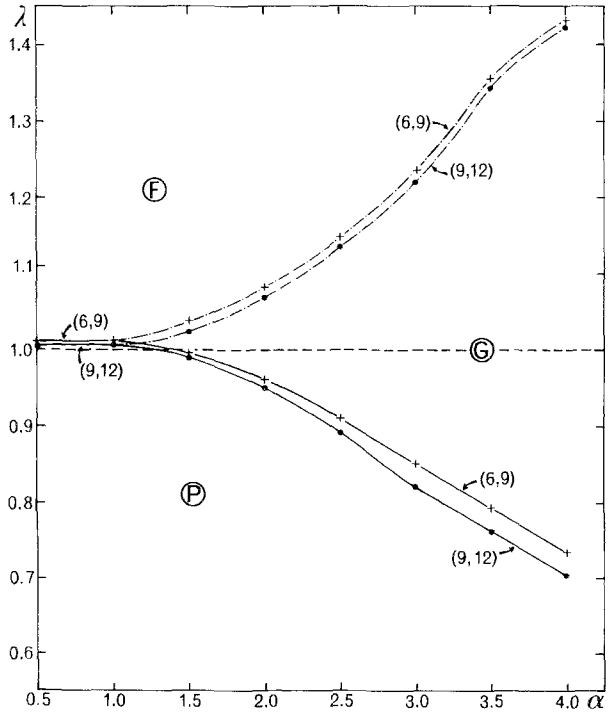

Fig. 4. Phase diagram of Hamiltonian (4.3).

Table II. Phenomenological Renormalization Estimates of Critical Couplings Obtained from Chains of Length L and $L-3$ Sites (see test)

L	$\alpha=0.5$		$\alpha=1.0$	$\alpha=1.5$		$\alpha=4.0$	
	$\lambda_c^1(L)$	$\lambda_c^2(L)$	$\lambda_c^1(L)=\lambda_c^2(L)$	$\lambda_c^1(L)$	$\lambda_c^2(L)$	$\lambda_c^1(L)$	$\lambda_c^2(L)$
6	1.016646	1.052010	1.056100	1.035964	1.098402	0.837525	1.535687
9	1.012998	1.009578	1.011965	0.997671	1.034407	0.738727	1.436336
12	1.004741	1.003270	1.004908	0.992996	1.021309	0.711854	1.430845
15	1.002270	1.001459	1.002632	0.992061	1.016182	0.704748	1.429352
18	1.001273	1.000764	1.001640	0.991925	1.013578	0.702653	1.428240
Extrapolated estimate	1.00003	1.00002	1.00008	0.99188	1.0074	0.70178	1.4249

while Table II lists, for selected values of α, estimates resulting from pairs of larger lattices together with extrapolated values obtained by using van den Broeck–Schwartz approximants.[19,20] Evidently, the (9, 12) estimate of the critical curve shown in Fig. 4 is almost indistinguishable, on the scale of the figure, from the true curve.

Figure 4 clearly shows a bifurcation point on the critical curve, at which a new intermediate phase appears in exactly the same fashion as occurs in the quantum Ashkin–Teller model.[16,21] It is also clear, from our finite-lattice data, that for fixed λ

$$\begin{aligned} G_L^1(\alpha) &< G_L^2(\alpha) \qquad \text{for} \quad \alpha < 1 \\ G_L^1(\alpha) &> G_L^2(\alpha) \qquad \text{for} \quad \alpha > 1 \\ G_L^1(\alpha) &= G_L^2(\alpha) \qquad \text{for} \quad \alpha = 1 \end{aligned} \tag{5.4}$$

Moreover, for given α, the estimators $\lambda_c^i(L)$ always decrease as the lattice size increases; these results strongly suggest that for $0 < \alpha \leqslant 1$ the transition is unique, occurring at the self-dual point $\lambda_c = 1$, while for $\alpha > 1$ there are two phase transitions. A similar finite-size analysis[21] of the quantum Ashkin–Teller model reveals that the relations (5.4) are also true for its two mass gaps, the four-state Potts model being the point at which the two gaps become degenerate and the critical line bifurcates. This similarity between the uniform case $\alpha = 1$ and the four-state Potts model supports the conjecture[7–11] that both models are in the same universality class.

To characterize the phases in Fig. 4, we observe that G^1 is associated with the correlation function between spins in sublattice $\bigcirc$ or $\diamond$, $\langle \sigma_{\bigcirc}^z(0)\, \sigma_{\bigcirc}^z(r) \rangle$, $\langle \sigma_{\diamond}^z(0)\, \sigma_{\diamond}^z(r) \rangle$, while G^2 is related to that between spins in sublattice $\square$, $\langle \sigma_{\square}^z(0)\, \sigma_{\square}^z(r) \rangle$. As a consequence, three phases can be distinguished:

1. A paramagnetic (P) phase (large λ), where

$$\langle \sigma^z_{\bigcirc} \rangle = \langle \sigma^z_{\square} \rangle = \langle \sigma^z_{\diamond} \rangle = 0 \tag{5.5}$$

and the full symmetry $Z(2) \otimes Z(2)$ is present.

2. A ferromagnetic (F) phase (small λ), where

$$\langle \sigma^z_{\bigcirc} \rangle \neq 0, \qquad \langle \sigma^z_{\square} \rangle \neq 0, \qquad \langle \sigma^z_{\diamond} \rangle \neq 0 \tag{5.6}$$

and all sublattices are ordered, the symmetry being totally broken.

3. A partially ordered (G) phase, where

$$\langle \sigma^z_{\square} \rangle \neq 0, \qquad \text{but} \qquad \langle \sigma^z_{\diamond} \rangle = 0, \qquad \langle \sigma^z_{\bigcirc} \rangle = 0 \tag{5.7}$$

and a partial $Z(2)$ symmetry remains corresponding to global transformations of the sublattices $\bigcirc$ and $\diamond$.

We turn now to the nature of the (continuous) transition that occurs at the various critical curves identified by the preceding analysis. We consider first the behavior (as a function of L) of the β-function[17,22]

$$\beta^i_L(\lambda, \alpha) = -G^i_L(\lambda, \alpha)/[G^i_L(\lambda, \alpha) - 2\lambda G^i_{L,\lambda}(\lambda, \alpha)], \qquad i = 1, 2 \tag{5.8}$$

where $G^i_{L,\lambda} = \partial G^i_L / \partial \lambda$. If, on an infinite lattice, the gap $G^i_\infty(\lambda, \alpha)$ vanishes as λ approaches $\lambda_c(\alpha)$ as

$$G^i_\infty(\lambda, \alpha) \sim [\lambda - \lambda_c(\alpha)]^\nu \tag{5.9}$$

then by finite-size scaling[17]

$$\beta_{L,c} \equiv \beta^i_L(\lambda_c(\alpha), \alpha) \sim AL^{-1/\nu} \tag{5.10}$$

as $L \to \infty$. Hence, a suitable estimator for the exponent ν is

$$y_L = -\frac{\ln(\beta^i_{L,c}/\beta^i_{L-3,c})}{\ln[L/(L-3)]} \to \frac{1}{\nu} \qquad \text{as} \quad L \to \infty \tag{5.11}$$

For $\alpha < 1$, one could, in principle, use both G^1 and G^2 to define β-functions. However, for numerical convenience we have considered only G^1. In addition, for $\alpha < 1$ we assumed $\lambda_c = 1$, while for $\alpha > 1$ we used the extrapolated values of the estimators obtained by phenomenological renormalization (see Table II).

A typical set of results (for $\alpha = 0.2$) is shown in Table III. The sequence of estimates obtained from (5.11), shown in the second column, is

Table III. β-Function Estimates of 1/ν for α = 0.2

L	y_L	Three-point
6	1.3420	—
9	1.1949	—
12	1.1566	1.1259
15	1.1412	1.1209
18	1.1331	1.1169
alt-ε alg	1.1035	—
θ alg	1.1125	—

clearly monotonic decreasing, but unfortunately relatively short. Assuming, which is reasonable on the basis of finite-size scaling,[17] that

$$y_L = 1/\nu + O(L^{-t}) \tag{5.12}$$

we have attempted to extrapolate these estimates of $1/\nu$ by the alternating ε algorithm[20,23] and the θ algorithm,[23,24] both of which are designed to accelerate sequences converging as in (5.12). In addition, we have tried to extract the limit y_∞ $(=1/\nu)$ by three-point fits[25] of the y_L,

$$y_L = y_\infty + b/L^t \tag{5.13}$$

Unfortunately, the brevity of the finite-lattice data results in some disparity among these various extrapolation procedures. However,

$$1/\nu = 1.12 \pm 0.02 \qquad (\alpha = 0.2) \tag{5.14}$$

would appear to be a conservative but reliable estimate. The corresponding final estimates for some other values of α are given in Table IV.

It is apparent from Table IV that, as in the quantum Ashkin–Teller model, the critical exponent ν is a continuous function of the coupling α. For α small, ν appears to approach the Ising value $(\nu = 1)$, which is consistent with the discussion in Section 2.[4] Also, for $\alpha > 4$, estimators of ν tend toward the Ising value, suggesting that the two phase transitions that occur for $\alpha > 1$ are Ising-like. Around $\alpha = 1$ convergence is poor, as occurs[21] in the Ashkin–Teller model around the four-state Potts model point.

[4] It is important, however, to note that the limiting case $K_0 \to \infty$ in (2.1), where the model is equivalent to a two-decoupled-Ising model, corresponds in (4.3) to the limit $\alpha \to 0$, and not $\alpha = 0$, where the system does not in fact have a phase transition.

Table IV. Extrapolated Estimates of 1/v

	1/v	
α	Estimate	Conjecture[a]
0.01	1.02	1.0063
0.2	1.12	1.1136
0.5	1.26	5/4
1.0	1.37[b]	3/2
$4.0(\lambda_c^1)$	0.98	1
$4.0(\lambda_c^2)$	1.05	1

[a] $1/\nu = 1 - \pi/[2\cos^{-1}(-\alpha)]$ (see text).
[b] From Ref. 11.

These results for ν induced us to conjecture that ν for (4.3) is given as a function of α by a similar relation as in the Ashkin–Teller model,[16] namely

$$1/\nu(\alpha) = 2 - \pi/[2\cos^{-1}(-\alpha)] \tag{5.15}$$

The conjectured values in Table IV were obtained from this formula. We discuss this point further in the next section.

6. MASS GAP AMPLITUDES

Statistical mechanical systems at criticality are believed to be conformally invariant.[26–28] In two dimensions, this assumption is particularly significant (for a recent review see Ref. 28). Specifically, Cardy[29,30] has derived a set of remarkable relations between the eigenvalue spectrum of the transfer matrix in a strip of finite width and the anomalous dimensions of the operator algebra describing the critical behavior of the infinite system. These results can be transcribed[31] to the quantum Hamiltonian formalism in which we are interested.[5]

The pertinent results for our purposes are as follows. Corresponding to each primary operator ϕ in the operator algebra of the infinite system there exists a set of eigenstates of the quantum Hamiltonian on a periodic chain of L sites with energies for $\lambda = \lambda_c$ given by

$$E_{n,n'} = E_0 + (2\pi/L)\,\zeta(x_\phi + n + n') + o(L^{-1}), \qquad n, n' = 0, 1, 2, \ldots \tag{6.1}$$

[5] For a discussion of the validity of the assumption of conformal invariance itself for a model such as (2.1) or (4.3) with mixed interactions see Ref. 11.

as $L \to \infty$, where x_ϕ is the anomalous dimension of ϕ. The constant ζ is unity in the transfer matrix formalism, but in the Hamiltonian case is model-dependent, reflecting the fact that the singular behavior of the Hamiltonian is insensitive to multiplication of H by a arbitrary constant.[21,31-34] The primary operators that appear in (6.1) are those governing the possible correlation functions.

Consider now the Hamiltonian (4.3). We can identify the lower mass gap amplitudes with the primary relevant operators as follows. The energy operator is related to the first excited state in the ground-state sector, i.e.,

$$G_L^0 = E_1(+\,+) - E_0(+\,+) = 2\pi\zeta x_\varepsilon / L + o(L^{-1}) \tag{6.2}$$

where $x_\varepsilon = 2 - 1/\nu$ is the dimension of the energy operator. There are two order operators for this system, one governing the sublattice $\square$ and the other governing sublattices $\diamond$ and $\bigcirc$. As discussed earlier, they are related to the sectors ($\mathscr{P}_1 = -1$, $\mathscr{P}_1 = +1$) and ($\mathscr{P}_1 = -1$, $\mathscr{P}_2 = -1$), respectively, leading to the identification

$$G_L^1 = E_0(-\,+) - E_0(+\,+) = 2\pi\zeta x_{\bigcirc} / L + o(L^{-1}) \tag{6.3}$$

$$G_L^2 = E_0(-\,-) - E_0(+\,+) = 2\pi\zeta x_{\square} / L + o(L^{-1}) \tag{6.4}$$

where $x_{\bigcirc}$ and $x_{\square}$ are the dimensions of the two operators.

It is interesting to observe that as a consequence of the existence of these different operators, the Hamiltonian (4.3) responds differently to magnetic fields $h_{\square}$ and $h_{\bigcirc}$ applied to sublattices $\square$ and $\bigcirc$ (or $\diamond$), respectively. In particular, the singular parts of the susceptibilities associated with these fields behave as

$$\partial^2 E_0 / \partial^2 h_{\square} |_{h_{\square}=0} \sim (\lambda - \lambda_c)^{-\gamma_{\square}} \tag{6.5}$$

and

$$\partial^2 E_0 / \partial^2 h_{\bigcirc} |_{h_{\bigcirc}=0} \sim (\lambda - \lambda_c)^{-\gamma_{\bigcirc}} \tag{6.6}$$

where $\gamma_{\square}$ and $\gamma_{\bigcirc}$ are related to $x_{\square}$ and $x_{\bigcirc}$ through

$$x_{\square} = \tfrac{1}{2}(2 - \gamma_{\square}/\nu), \qquad x_{\bigcirc} = \tfrac{1}{2}(2 - \gamma_{\bigcirc}/\nu) \tag{6.7}$$

In order to extract the anomalous dimensions from finite-lattice data and equations (6.2)–(6.4), we need to calculate the constant ζ. This can be done from the difference between higher energy states associated with the same primary operator.[31] For example, in the sector ($\mathscr{P}_1 = -1$, $\mathscr{P}_2 = +1$), the difference

$$Z_L = E_1(-\,+) - E_0(-\,+) = 2\pi\zeta / L + o(L^{-1}) \tag{6.8}$$

where $E_1(-+)$ is the lowest energy with nonzero momentum. In practice for $\alpha \leqslant 1$, we estimated x_ε, $x_\square$, and $x_\bigcirc$ by forming the ratios

$$r_\varepsilon(L) = G_L^0/Z_L, \qquad r_\bigcirc(L) = G_L^1/Z_L, \qquad r_\square(L) = G_L^2/Z_L \tag{6.9}$$

where all energies were evaluated at $\lambda = 1$.[6] From (6.2)–(6.4) and (6.8) we expect

$$r_\varepsilon(L) \to x_\varepsilon, \qquad r_\bigcirc(L) \to x_\bigcirc, \qquad r_\square(L) \to x_\square \tag{6.10}$$

respectively, as $L \to \infty$. The limits were numerically estimated by fitting r's for three successive lattices to

$$r(L) = x + a/L^t \tag{6.11}$$

Table V summarizes this analysis for $\alpha = 0.2$. The convergence is extremely good, leading to the confident estimates of

$$x_\varepsilon = 0.885 \pm 0.005, \quad x_\bigcirc = 0.126 \pm 0.002, \quad x_\square = 0.222 \pm 0.002 \tag{6.12}$$

The results of corresponding analyses for other values of α are shown in Table VI, the convergence deteriorating as α approaches unity. These results clearly establish that for $\alpha \leqslant 1$, x_ε and $x_\square$ are functions of α (approaching Ising values as $\alpha \to 0$), while $x_\bigcirc$ is constant. In addition, the ratio $x_\square/(2x_\bigcirc x_\varepsilon)$ appears to be almost constant (~ 1) for all α.

The similarity between the results of Table VI and those of the quantum Ashkin–Teller model[21] is complete if we identify the pair $(x_\bigcirc, y_\bigcirc)$ with the anomalous dimension x_m of the magnetization operator and the

[6] The required energy levels were computed by the Lanczos algorithm from appropriately selected initial states (see Refs. 11 and 34). Some care (and numerical experimentation) is necessary to ensure that any particular initial state yields the successive eigenenergies of the sets (6.1).

Table V. Extrapolation of Mass Gap Amplitude Ratios for $\alpha = 0.2$

L	$r_\varepsilon(L)$	Three-point fit	$r_\bigcirc(L)$	Three-point fit	$r_\square(L)$	Three-point fit
6	1.3086	—	0.2027	—	0.3580	—
9	1.0386	—	0.1527	—	0.2695	—
12	0.8946	0.3522	0.1293	0.0723	0.2282	0.1276
15	0.8901	0.8897	0.1277	0.1275	0.2253	0.2248
18	0.8876	0.8816	0.1269	0.1250	0.2238	0.2205

Table VI. Anomalous Dimensions for Hamiltonian (4.21)

	x_ε		$x_\bigcirc$		$x_\square$	
α	Estimate[a]	Conjecture[b]	Estimate[a]	Conjecture[b]	Estimate[a]	Conjecture[b]
0.01	0.999	0.99367...	0.125	1/8	0.248	0.24842...
0.1	0.938	0.94005...	0.125	1/8	0.235	0.23501...
0.2	0.885	0.88638...	0.126	1/8	0.222	0.22159...
0.4	0.780	0.79241...	0.125	1/8	0.196	0.19810...
0.5	0.740	3/4	0.125	1/8	0.183	3/16
0.8	0.632	0.62880...	0.123	1/8	0.148	0.15720...
1.0[c]	0.63	1/2	0.13	1/8	0.13	1/8
3.0(λ_c^1)	1.00	1	0.125	1/8	—	—
3.0(λ_c^2)	1.02	1	—	—	0.13	1/8
4.0(λ_c^1)	1.00	1	0.127	1/8	—	—
4.0(λ_c^2)	1.01	1	—	—	0.122	1/8

[a] Numbers quoted are central estimates with (subjective) errors of $\pm(2\text{–}5)$ in the last digit [cf. Eq. (6.12)].
[b] See Eqs. (6.14)–(6.16).
[c] See Ref. 11. (For $\alpha = 1$, $x_{\square}$ and $x_\bigcirc$ are equal by symmetry.)

critical exponent γ_m of the magnetic susceptibility, respectively, and the pair $(x_\square, \gamma_\square)$ with the dimension x_p of the electric polarization operator and the critical exponent γ_p of the electric susceptibility. As a consequence of this correspondence, our results suggest the following conjecture for the critical indices of (4.3) for $\alpha \leqslant 1$:

$$x_\varepsilon = 2 - 1/\nu = \pi/2 \cos^{-1}(-\alpha) \tag{6.13}$$

$$x_\bigcirc = 1/8 \tag{6.14}$$

$$x_\square = x_\varepsilon/4 \tag{6.15}$$

In Table VI these are the "conjectured" values. The agreement with the actual numerical estimates is gratifying.

For $\alpha > 1$, the results of Table VI are consistent with both transitions being Ising-like. The apparently poorer agreement can be attributed at least in part to errors in the location of the critical couplings of the infinite lattice. The extrapolated critical coupling for $\alpha = 4$ is given in Table II, while for $\alpha = 3$ these values are $\lambda_c^1(\infty) = 0.79929$ and $\lambda_c^2(\infty) = 1.25157$.

In addition to these predictions for mass gap amplitudes that have been exploited above, conformal invariance also predicts[35,36] that the ground-state energy of H at $\lambda = \lambda_c$ should behave as

$$E_0/L = e_0 - \tfrac{1}{6}\pi c\zeta/L^2 + o(L^{-2}) \tag{6.16}$$

Table VII. Estimates of Conformal Anomaly

a	$b=\pi c\zeta/6$	$z=2\pi\zeta$	c
0.1	0.221	2.648	1.002
0.2	0.434	5.20	1.00
0.4	0.823	9.86	1.00
0.8	1.45	18.0	0.97
1.0	1.68	20.3	1.00
$3.0(\lambda_c^1)$	1.3	64	0.49
$3.0(\lambda_c^2)$	1.6	80	0.48
$4.0(\lambda_c^1)$	1.41	66.8	0.507
$4.0(\lambda_c^2)$	2.00	95.0	0.505

as $L\to\infty$, where e_0 is the infinite-lattice value and c is the central charge or conformal anomaly of the appropriate conformal class of the transition in the bulk system.[28,37] Hence, finite-lattice calculations can, in principle, allow c to be directly estimated.

In practice, the extraction of c from finite-lattice data is delicate because of the necessity of estimating the (unknown) infinite-lattice limit e_0 and also, for a quantum Hamiltonian, of independently estimating the constant ζ. We have attempted to estimate c by fitting (i) data for $E_0(L)$ from two successive lattices to

$$E_0(L)=Le_0-b/L \tag{6.17}$$

and (ii) the sequence (6.8) to

$$LZ_L=z+w/L^t \tag{6.18}$$

using data from three lattices. An estimate of the conformal anomaly c is then given by

$$c=12b/z \tag{6.19}$$

and is tabulated in Table VII.

For $\alpha\leqslant 1$, the estimates of c are slightly larger than the value of $c=1$ expected for a line of continuously varying critical exponents.[37] Given the numerical difficulties in extracting c, we do not place any emphasis on this discrepancy. On the other hand, for $\alpha>1$ the estimate of c is dramatically different and consistent with that of the Ising model,[37] namely $c=1/2$. This change in the value of c as α passes through $\alpha=1$ is identical to that found in the Ashkin–Teller model.[38,39]

7. CONCLUSION AND SUMMARY

In this paper we have studied the three-spin quantum Hamiltonian

$$-H(\lambda, \alpha) = \sum_i [(\sigma^z_{3i}\sigma^z_{3i+1}\sigma^z_{3i+2} + \alpha\sigma^z_{3i+1}\sigma^z_{3i+2}\sigma^z_{3i+3} + \alpha\sigma^z_{3i+2}\sigma^z_{3i\pm+2}\sigma^z_{3i+4}) \times \lambda(\alpha\sigma^x_{3i} + \sigma^x_{3i+1} + \alpha\sigma^x_{3i+2})] \tag{7.1}$$

Our study clearly indicates that the phase diagram of this model has the same topology as that of the quantum Ashkin–Teller model. For $\alpha \leqslant 1$, a single phase transition occurs at the self-dual point $\lambda = \lambda_c = 1$ with critical indices conjectured to be given by

$$x_\varepsilon = 2 - 1/\nu = \pi/2 \cos^{-1}(-\alpha) \tag{7.2}$$

$$x_\square = 1/8 \tag{7.3}$$

$$x_\bigcirc = x_\varepsilon/4 \tag{7.4}$$

while for $\alpha > 1$ two phase transitions in the universality class of the Ising model appear. From our generalized quantum model it is clear that the uniform model $\alpha = 1$ belongs to the same universality class as the four-state Potts model and Baxter–Wu model, clarifying earlier controversial conclusions about this point, the poor convergence reported in various studies[7–11] being a consequence of the well-known marginal effects at the four-state Potts model.

Finally, we would like to mention that although our numerical analysis has been performed in the Hamiltonian formalism, we believe that the same critical behavior is shared by the classical model (4.1) and the classical Ashkin–Teller model.

ACKNOWLEDGMENTS

This work was supported in part by the Australian Research Grant Scheme and by Fundação de Amparo à Pesquisa do Estado de São Paulo, Brazil.

REFERENCES

1. R. J. Baxter, *Ann. Phys.* (N.Y.) **70**:193–228 (1972).
2. J. Ashkin and E. Teller, *Phys. Rev.* **64**:178–184 (1943).
3. R. J. Baxter, *Exactly Solved Models in Statistical Mechanics* (Academic Press, London, 1982).
4. R. J. Baxter and F. Y. Wu, *Phys. Rev. Lett.* **31**:1294–1297 (1973).

5. M. N. Barber, *Phys. Rep.* **59**:375–409 (1980).
6. R. V. Ditzian, J. R. Banavar, C. S. Grest, and L. P. Kadanoff, *Phys. Rev. B* **22**:2542–2553 (1980).
7. J. M. Debierre and L. Turban, *J. Phys. A: Math. Gen.* **16**:3571–3584 (1983).
8. K. A. Penson, R. Jullien, and P. Pfeuty, *Phys. Rev. B* **26**:6334–6337 (1982).
9. L. Turban, *J. Phys. Lett. (Paris)* **43**:L259–265 (1982).
10. F. Iglói, D. V. Kapor, M. Škrinjar, and J. Sólyon, *J. Phys. A: Math. Gen.* **16**:4067–4071 (1983).
11. F. C. Alcaraz and M. N. Barber, *J. Phys. A: Math. Gen.* **20**, in press.
12. T. M. Schultz, E. Lieb, and D. Mathis, *Rev. Mod. Phys.* **36**:856 (1964); J. B. Kogut, *Rev. Mod. Phys.* **51**:659–713 (1979).
13. H. A. Kramers and G. H. Wannier, *Phys. Rev.* **60**:252 (1941).
14. R. Savit, *Rev. Mod. Phys.* **52**:453–487 (1980).
15. E. Fradkin and L. Susskind, *Phys. Rev. D* **17**:2637–2658 (1978).
16. M. Kohmoto, M. den Nijs, and L. P. Kadanoff, *Phys. Rev. B* **24**:5229–5241 (1981).
17. M. N. Barber, in *Phase Transitions and Critical Phenomena*, Vol. 8, C. Domb and J. L. Lebowitz, eds. (Academic Press, London, 1983), p. 143.
18. M. P. M. Nightingale, *J. Appl. Phys.* **53**:7927 (1982).
19. J. M. van den Broeck and L. W. Schwartz, *SIAM J. Math. Anal.* **10**:658 (1979).
20. C. J. Hamer and M. N. Barber, *J. Phys. A: Math. Gen.* **14**:2009–2025 (1981).
21. F. C. Alcaraz and J. R. Drugowich de Felício, *J. Phys. A: Math. Gen.* **17**:L651–655 (1984).
22. C. J. Hamer, J. Kogut, and L. Susskind, *Phys. Rev. D* **19**:3091–3105 (1979).
23. M. N. Barber and C. J. Hamer, *J. Aus. Math. Soc. B* **23**:229–240 (1982).
24. D. A. Smith and W. F. Ford, *SIAM J. Num. Anal.* **16**:223–240 (1979).
25. H. W. J. Blöte and M. P. Nightingale, *Physica* **112A**:405 (1982).
26. A. M. Polyakov, *Sov. Phys. JETP Lett.* **12**:381 (1970).
27. A. A. Belavin, A. M. Polyakov, and A. B. Zamolodchikov, *J. Stat. Phys.* **34**:763 (1984); *Nucl. Phys. B* **241**:333 (1984).
28. J. L. Cardy, in *Phase Transitions and Critical Phenomena*, C. Domb and J. L. Lebowitz, eds. (Academic Press, in press).
29. J. L. Cardy, *J. Phys. A: Math. Gen.* **17**:L385–357 (1984).
30. J. L. Cardy, *Nucl. Phys. B* **270** [FS16]:186 (1986).
31. G. v. Gehlen, V. Rittenberg, and H. J. Ruegg, *J. Phys. A: Math. Gen.* **19**:107–119 (1985).
32. K. A. Penson and M. Kolb, *Phys. Rev. B* **29**:2854–2856 (1984).
33. F. C. Alcaraz, J. R. Drugowich de Felício, R. Köberle, and F. Stick, *Phys. Rev. B* **32**:7469–7475 (1985).
34. F. C. Alcaraz and J. R. Drugowich de Felício, *Rev. Bras. Fís.* **15**:128–141 (1985).
35. H. W. J. Blöte, J. C. Cardy, and M. P. Nightingale, *Phys. Rev. Let.* **56**:742–745 (1986).
36. I. Affleck, *Phys. Rev. Lett.* **56**:746–748 (1986).
37. D. Friedan, Z. Qiu, and S. Shenker, *Phys. Rev. Lett.* **52**:1575(1984).
38. G. v. Gehlen and V. Rittenberg, *J. Phys. A: Math. Gen.* **20**, in press.
39. J. R. Drugowich de Felício, private communication